

LETTERS

Tropical cyclones and permanent El Niño in the early Pliocene epoch

Alexey V. Fedorov¹, Christopher M. Brierley¹ & Kerry Emanuel²

Tropical cyclones (also known as hurricanes and typhoons) are now believed to be an important component of the Earth's climate system^{1–3}. In particular, by vigorously mixing the upper ocean, they can affect the ocean's heat uptake, poleward heat transport, and hence global temperatures. Changes in the distribution and frequency of tropical cyclones could therefore become an important element of the climate response to global warming. A potential analogue to modern greenhouse conditions, the climate of the early Pliocene epoch (approximately 5 to 3 million years ago) can provide important clues to this response. Here we describe a positive feedback between hurricanes and the upper-ocean circulation in the tropical Pacific Ocean that may have been essential for maintaining warm, El Niño-like conditions^{4–6} during the early Pliocene. This feedback is based on the ability of hurricanes to warm water parcels that travel towards the Equator at shallow depths and then resurface in the eastern equatorial Pacific as part of the ocean's wind-driven circulation^{7,8}. In the present climate, very few hurricane tracks intersect the parcel trajectories; consequently, there is little heat exchange between waters at such depths and the surface. More frequent and/or stronger hurricanes in the central Pacific imply greater heating of the parcels, warmer temperatures in the eastern equatorial Pacific, warmer tropics and, in turn, even more hurricanes. Using a downscaling hurricane model^{9,10}, we show dramatic shifts in the tropical cyclone distribution for the early Pliocene that favour this feedback. Further calculations with a coupled climate model support our conclusions. The proposed feedback should be relevant to past equable climates and potentially to contemporary climate change.

The response of tropical cyclones to global climate change, and their role in climate, has been a subject of much debate^{1,2,11}. The role of hurricanes in past climates has also been discussed, especially in relation to 'hothouse' climates such as that of the Eocene epoch^{3,12,13}. The motivation for this study originates in the climate of the early Pliocene—an epoch that many consider the closest analogue to future greenhouse conditions¹⁴. The external factors that control climate, including continental geography and the intensity of sunlight incident on the Earth, were essentially the same as at present. The atmospheric concentration of carbon dioxide was in the range 300–400 p.p.m. (ref. 15), similar to current, elevated values. Yet, the climate was significantly warmer then. Evidence from PRISM (the Pliocene research, interpretation and synoptic mapping project^{16–19}) indicates mid-Pliocene global mean temperatures 2–3 °C warmer than today. The early Pliocene was approximately 4 °C warmer than today²⁰.

The tropical climate then was also markedly different from the present-day climate. In particular, the Pacific developed a permanent El Niño-like state (for a review, see ref. 6). This term implies that the mean sea surface temperature (SST) gradient along the Equator was

very weak or absent (Fig. 1a). Similarly, the meridional temperature gradient from the Equator to the mid-latitudes was significantly reduced²¹. In fact, in the early Pliocene the SST distribution was virtually flat between the Equator and the subtropics, indicating a poleward expansion of the ocean warm pool (Fig. 1b). Cold surface waters were almost absent from upwelling zones off the western coasts of Africa and the Americas^{22,23}.

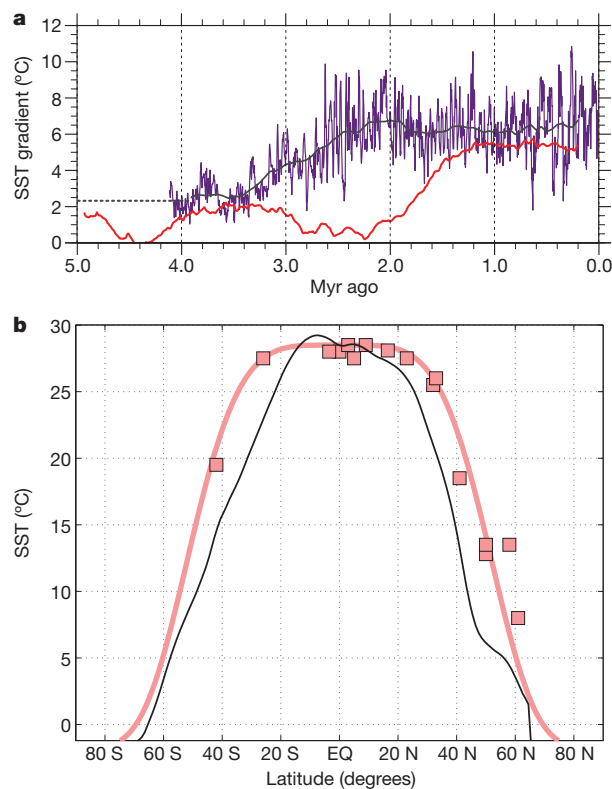


Figure 1 | Changes in SSTs in the Pacific over the past ~5 million years. **a**, The development of the meridional SST contrast in the tropical East Pacific (purple line²¹) and the zonal SST gradient along the Equator (red line³). The meridional temperature difference is estimated from alkenone records from ODP sites 846 (3° S, 91° W) and 1012 (32° N, 118° W). The zonal temperature difference is calculated from Mg/Ca temperature records from ODP sites 806 (0° N, 159° E) and 847 (0° N, 95° W). The black and the red lines are obtained using a 400,000-year running mean. **b**, A reconstruction of the latitudinal SST distribution in the early Pliocene (~4 million years ago) in the mid-Pacific roughly along the Date Line (pink squares), after ref. 21. The pink line shows the hypothetical fit of equation (1) of Methods to the proxy data. The black line shows the modern climatological SSTs along 180° E.

¹Department of Geology and Geophysics, Yale University, New Haven, Connecticut 06520, USA. ²Department of Earth, Atmospheric, and Planetary Sciences, MIT, Cambridge, Massachusetts 02139, USA.

A major unresolved issue is how the early Pliocene climate—and especially its tropical conditions—were maintained, given that CO₂ concentrations were very similar to modern values. So far, climate models have not been able to reproduce the tropical SST patterns characteristic of the early Pliocene^{18,24}. A recent study²¹ has suggested that additional mechanisms, perhaps related to ocean vertical mixing, should be considered in order to simulate a tropical climate state with weak SST contrasts. Could tropical cyclones provide such a mechanism?

Tropical storms are known to increase ocean vertical mixing—in the wake of hurricanes, the ocean mixed layer can deepen to 120–200 m (refs 13, 25, 26). As little is known about hurricanes in the past²⁷, here we reconstruct hurricane characteristics by completing several successive steps, including (1) reconstructing the SST field; (2) modelling the large-scale atmospheric circulation with a general circulation model (GCM); and (3) using the GCM data to drive a statistical downscaling model (SDSM), which computes synthetic hurricane tracks and intensity (Methods Summary; Methods).

The ocean temperature field is the starting point for our analysis, as the most reliable climatic information for the early Pliocene comes as SST data. Following ref. 21, we take the SST distribution in Fig. 1b, interpolate the data with a continuous function and, assuming very small east–west SST variations, extend the SST profile zonally. The SST profile is shifted along the meridian following the progression of the modern annual cycle. The resulting SST field is then used as boundary conditions for the atmospheric GCM (CAM3, T85 spectral resolution, see Methods).

GCM calculations show an atmospheric circulation for the early Pliocene with weaker (meridional) Hadley and (zonal) Walker cells²¹—the weakened atmospheric circulation implies reduced vertical wind shear, which is favourable for tropical cyclones. Next, we use the large-scale climatological atmospheric flow from these calculations to drive the downscaling model: weak atmospheric vortices are randomly seeded over the ocean and their evolution is followed by

the SDSM. The model predicts the tracks and calculates the intensity of the vortices—most of these disturbances die out, but some develop into mature tropical cyclones.

The results for the modern and early Pliocene climates are compared in Fig. 2 (and Supplementary Fig. 1). The SDSM adequately reproduces the observed modern distribution of tropical storms in the Pacific. The strongest modelled hurricane activity occurs east of the Philippines and Japan—a region known for frequent typhoons. Other active regions coincide with warm-water pools in the eastern North Pacific, the western South Pacific, and in the Indian Ocean. There are almost no hurricanes in the central Pacific or in the eastern South Pacific. In the North Atlantic, the tracks are shifted slightly towards the Caribbean, owing to biases in the winds simulated by the atmospheric GCM.

For the early Pliocene, the pattern of simulated tropical storm activity differs dramatically. Reduced vertical wind shear combined with warmer SSTs lead to a widespread increase in tropical cyclones (Supplementary Fig. 1). There are now two broad bands of cyclone activity both north and south of the Equator extending from the western to the eastern Pacific. Because of the warm pool's expansion, the lifespan of an average tropical cyclone is now 2–3 days longer. There are many more hurricanes in the South Pacific (and even a few in the South Atlantic). The overall number of hurricanes almost doubles (a smaller increase occurs when a lower-resolution atmospheric GCM, T42, is used). With reduced SST contrasts, the seasonal dependence of tropical cyclone activity becomes less pronounced, with cyclones occurring throughout the seasons.

How would these changes in hurricane activity influence the tropical climate? To answer this question, we first need to look at the upper ocean circulation in the tropics (Fig. 3a). This wind-driven circulation connects the regions of subduction off the coasts of California and Chile with the Equatorial Undercurrent and eventually with the eastern equatorial Pacific. The circulation is associated with a shallow ocean meridional overturning, with penetration

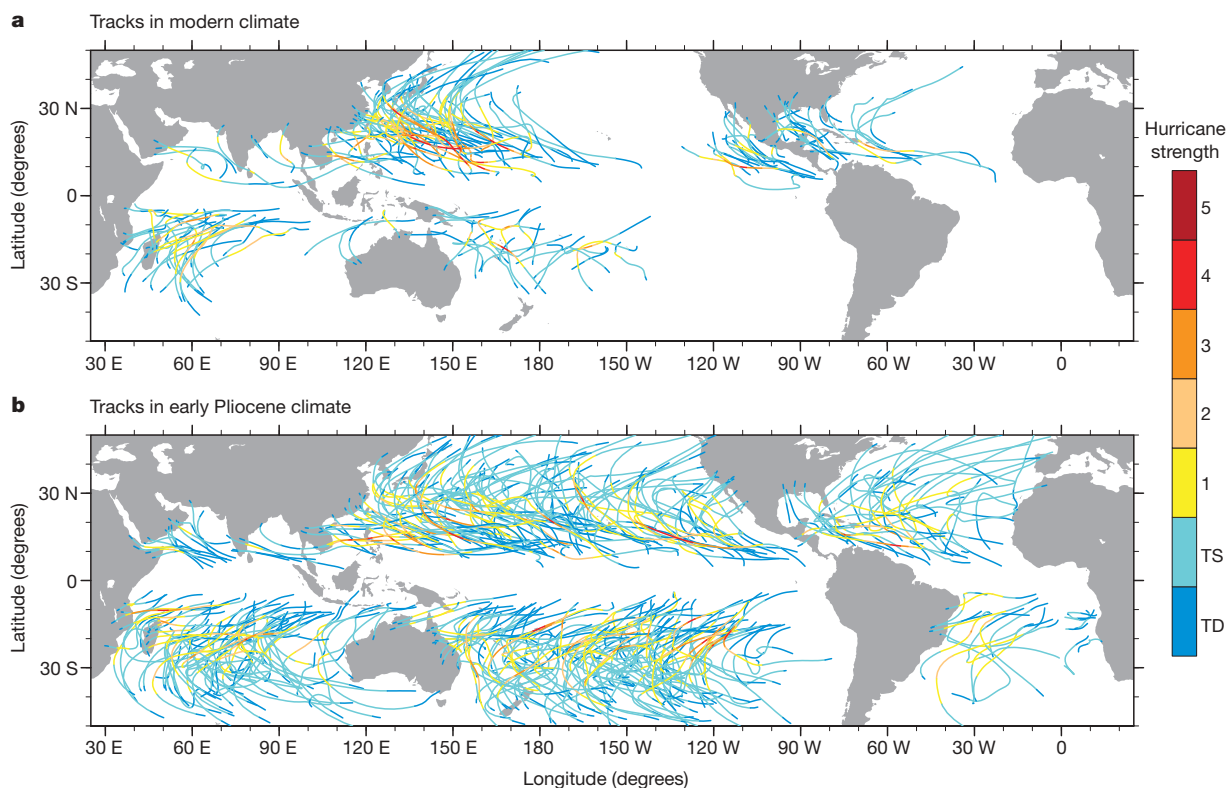


Figure 2 | The tracks of tropical cyclones simulated by the SDSM. **a**, In the modern climate, and **b**, in the early Pliocene climate. The colours indicate hurricane strength—from tropical depression (TD; blue) to tropical storm

(TS; cyan) to category-5 hurricanes (red). The tracks shown in each panel are a two-year subsample of 10,000 simulated tropical cyclones.

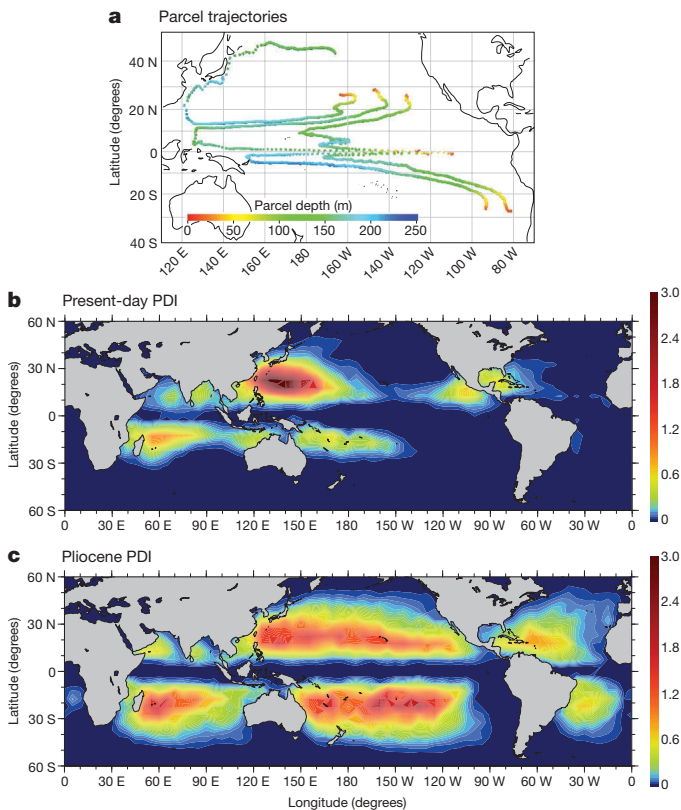


Figure 3 | Ocean wind-driven circulation and the PDI for tropical cyclones. **a**, The upper ocean circulation is shown as trajectories of water parcels over a period of 16 years after subduction off the coasts of California and Peru as simulated by an ocean GCM. The parcels move downward, westward and towards the Equator unless they start too far west off California, in which case they join the Kuroshio Current and the Pacific subtropical gyre. Along the Equator the parcels rise to the surface while being carried eastward by the Equatorial Undercurrent. The circulation remains shallow, with the parcel depth (indicated by colours) never exceeding 200–250 m. Adapted from refs 7 and 8. **b**, The PDI of the simulated tropical cyclones for modern conditions (in units of $\text{m}^3 \text{s}^{-2} \times 10^{10}$). Large values indicate regions where tropical cyclones can induce strong vertical mixing of the ocean. **c**, The same for the early Pliocene. Note the shift of the PDI towards the central Pacific, and much larger values south of the Equator during the Pliocene.

depths not greater than ~ 250 m, typically referred to as the shallow subtropical cells^{7,28}.

The effect of hurricanes on the ocean can be measured with the annual average power dissipation index (PDI), which approximates the amount of energy per unit area that tropical cyclones generate each year¹. A significant fraction of this energy is available to mix the upper ocean. In general, the PDI distribution coincides with the areas of strong hurricane activity, both in terms of frequency of occurrence and strength.

For the modern climate, the simulated mean PDI exhibits a strong maximum in the western tropical Pacific north of 10°N (Fig. 3b). Water parcels can travel towards the Equator after subduction through two ‘windows’ of the modern PDI distribution in the central Pacific without any interference from tropical storms (also see Supplementary Fig. 1). In the west Pacific, the parcels travel at the fringe of the PDI maximum, where the mixing can affect the Pacific subtropical gyre, but not the shallow subtropical cells.

For the early Pliocene, two bands of high PDI now cover the entire zonal extent of the Pacific (Fig. 3c), allowing interaction between the hurricanes and ocean circulation. With the two ‘windows’ closed, hurricane paths inevitably intersect the trajectories of water parcels, raising the parcels’ temperature. The end result is a warming of the eastern equatorial Pacific where the parcels rise to the surface. Ocean–atmosphere interactions²⁹ can amplify this warming via the

positive Bjerknes feedback—higher temperatures in the eastern equatorial Pacific imply weaker zonal winds, weaker equatorial upwelling and even higher temperatures in the east.

To test this hypothesis and replicate the effect of hurricanes for the early Pliocene, we have performed several numerical experiments with a coupled ocean–atmosphere GCM (CCSM3). In particular, we increase the ocean background vertical diffusivity tenfold to $\sim 1 \text{ cm}^2 \text{ s}^{-1}$ (consistent with ref. 3) above 200 m depth in two extra-tropical bands between 8° and 40° north and south of the Equator (similar to ref. 30). Simultaneously, CO_2 concentrations are increased from preindustrial (290 p.p.m.) to 1990 (355 p.p.m.) levels.

The tropical ocean response after 200 years of simulation includes (1) persistent El Niño-like warming in the central to eastern equatorial Pacific (Fig. 4b, Supplementary Fig. 2); (2) a small warming off the Equator indicative of a meridional expansion of the warm pool; (3) a temperature rise in most of the coastal upwelling regions; (4) a deepening of the ocean tropical thermocline; and (5) a reduction of the thermocline slope along the Equator in the Pacific (Supplementary Fig. 3). For comparison, we display SST changes in the same model (Fig. 4c) when only CO_2 concentrations are raised. In this case, the temperature increase is moderate (below 1°C) and almost uniform, indicating a near radiative-equilibrium response.

The warming of the eastern equatorial Pacific (the region typically referred to as the equatorial cold tongue) in response to increased extra-tropical mixing remains robust in a broad parameter range. Its magnitude depends on the specified diffusivity and the width of the equatorial gap between the two bands of enhanced mixing. The

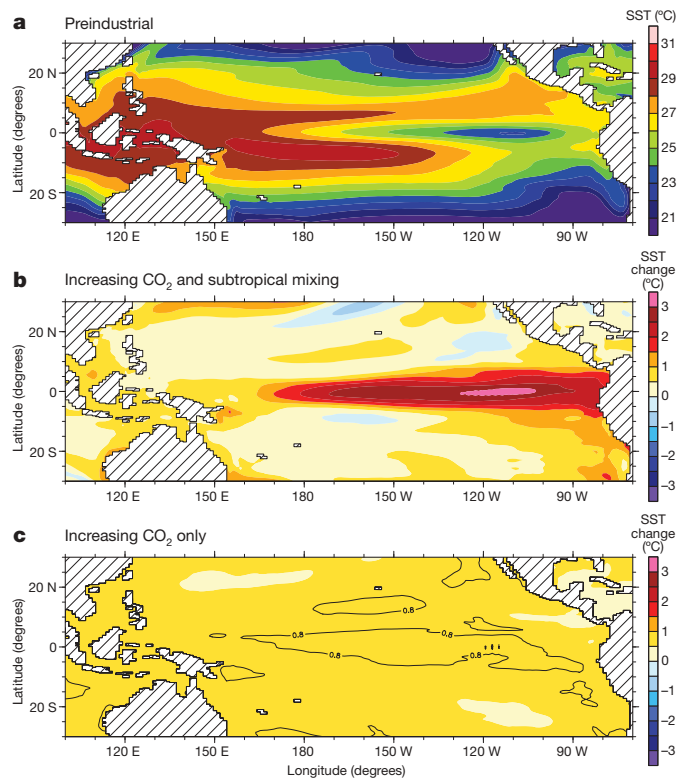


Figure 4 | SST changes in the tropical Pacific simulated by the coupled model. **a**, SSTs for preindustrial climate conditions; **b**, SST changes in response to increasing CO_2 concentration from 290 p.p.m. (preindustrial) to 355 p.p.m. (the level of 1990) and increasing vertical diffusivity in the upper ocean (0–200 m) in the extra-tropical bands (8° – 40° north and south of the Equator), after 200 years of calculations for the Pliocene scenario. The SST increase has a clear signature of permanent El Niño-like conditions, with the warming reaching 3.5°C in the eastern equatorial Pacific. **c**, SST changes in response to increasing CO_2 concentration alone. The SST increase is virtually uniform and remains below 1°C .

smaller the gap, the greater the warming that is achieved. The gap being fully closed wipes out the zonal SST gradient almost completely (Fig. 5). The depth of penetration of the mixing into the ocean is also important—the maximum warming occurs for depths of around 150–200 m.

Ocean adjustment to the imposed forcing involves different time-scales: from daily (ocean mixing from individual storms, not considered here) to seasonal, to decadal (the circulation time in the ocean's subtropical cell). The coupled model simulation takes nearly 100 years for the full impact of the imposed mixing to emerge (Fig. 5).

The results in Figs 2–5 suggest a plausible mechanism for sustaining the early Pliocene climate, based on the coupling between tropical SSTs, tropical cyclones and upper-ocean circulation. The expansion of the warm pool allows for enhanced hurricane activity throughout the subtropical Pacific. Stronger ocean vertical mixing in the two hurricane bands leads to further warming of the eastern equatorial Pacific and a deepening of the tropical thermocline. In turn, the warmer climate facilitates hurricane activity. This amounts to a positive feedback (Supplementary Fig. 4), which can potentially lead to multiple climate states—one with permanent El Niño-like conditions and strong hurricane activity, and the other corresponding to modern climate with a cold eastern equatorial Pacific.

Although promising, the proposed mechanism does not solve the early Pliocene problem completely, as the changes shown in Fig. 4b (and Supplementary Fig. 2) are not sufficient to fully bring the model to the reconstructed climate. Reduction in the meridional SST gradient is too weak compared to ref. 21, which may be related in part to biases in the coupled model (an excessively strong equatorial cold

tongue extends too far westward) or perhaps to still missing processes affecting the poleward heat transport. Numerical models able to simulate El Niño/Southern Oscillation and the mean state of the tropical Pacific more accurately are needed³¹. More work is required to improve our understanding of atmospheric dynamics in warmer climates³², and to better constrain the Pliocene SSTs^{20,21} and the contribution of tropical storms to ocean mixing^{3,12,13}. Resolving these issues will be critical both to model the early Pliocene climate and to predict future climate change, for which hurricane–ocean circulation feedbacks could become critical.

METHODS SUMMARY

The modelling of tropical storms in this study is performed using the SDSM^{9,10}. The first step of the downscaling process is to produce a global climatology for the vertical profiles of temperature, atmospheric humidity and winds. For this purpose, two experiments with an atmospheric GCM (CAM3, T85 resolution) are conducted—one forced with modern climatological SSTs, the other with an early Pliocene SST reconstruction²¹.

The next step is to create synthetic hurricane tracks. In order to increase track variations, self-consistent random realizations of the winds are created using the means, variances and covariances from the GCM simulations. Weak vortices are seeded at random throughout the tropics and their subsequent progression is computed using a model describing advection by the vertically averaged winds, corrected for a β -drift (poleward and westward motion that a hurricane would have in the absence of background winds because of the variation of Coriolis force with latitude). Over 20,000 synthetic cyclones were produced (only two years worth of tracks are shown in Fig. 2).

Once the tracks have been determined, an intensity model⁹ is integrated along each track (the Coupled Hurricane Intensity Prediction System, CHIPS). It is an axisymmetric atmosphere model with a parameterization of vertical wind shear, coupled to a simple one-dimensional ocean model, which captures the effect of the ocean mixed layer on tropical cyclones. In lieu of mixed layer depth reconstructions for the early Pliocene, we use present day values. We anticipate that the actual ocean mixed layer was deeper in the Pliocene, so that if anything we underestimate the strength of tropical storms.

The PDI in Fig. 3 is defined as an integral of v^3 over the duration of all tropical cyclones that occur on average in the course of 1 year in a $5^\circ \times 5^\circ$ gridbox (v is the maximum wind velocity associated with the cyclones in the gridbox). Further details of the SST reconstruction and numerical simulations are discussed in the Methods.

Full Methods and any associated references are available in the online version of the paper at www.nature.com/nature.

Received 8 July; accepted 29 December 2009.

1. Emanuel, K. Increasing destructiveness of tropical cyclones over the past 30 years. *Nature* **436**, 686–688 (2005).
2. Webster, P., Holland, G., Curry, J. & Chang, H. Changes in tropical cyclone number, duration, and intensity in a warming environment. *Science* **309**, 1844–1846 (2005).
3. Srivler, R. L. & Huber, M. Observational evidence for an ocean heat pump induced by tropical cyclones. *Nature* **447**, 577–580 (2007).
4. Molnar, P. & Cane, M. A. El Niño's tropical climate and teleconnections as a blueprint for pre-Ice Age climates. *Paleoceanography* **17**, 1021, doi:10.29/2001PA000663 (2002).
5. Wara, M. W., Ravelo, A. C. & Delaney, M. L. Permanent El Niño-like conditions during the Pliocene warm period. *Science* **309**, 758–761 (2005).
6. Fedorov, A. *et al.* The Pliocene paradox (mechanisms for a permanent El Niño). *Science* **312**, 1485–1489 (2006).
7. Gu, D. & Philander, S. Interdecadal climate fluctuations that depend on exchanges between the tropics and extratropics. *Science* **275**, 805–807 (1997).
8. Barreiro, M., Fedorov, A. V., Pacanowski, R. C. & Philander, S. G. Abrupt climate changes: how the freshening of the northern Atlantic affects the thermohaline and wind-driven oceanic circulations. *Annu. Rev. Earth Planet. Sci.* **36**, 33–58 (2008).
9. Emanuel, K., Ravelo, S., Vivant, E. & Risi, C. A statistical deterministic approach to hurricane risk assessment. *Bull. Am. Meteorol. Soc.* **87**, 299–314 (2006).
10. Emanuel, K., Sundararajan, R. & Williams, J. Hurricanes and global warming — results from downscaling IPCC AR4 simulations. *Bull. Am. Meteorol. Soc.* **89**, 347–367 (2008).
11. Knutson, T. R., Sirutis, J. J., Garner, S. T., Vecchi, G. A. & Held, I. M. Simulated reduction in Atlantic hurricane frequency under twenty-first-century warming conditions. *Nature Geosci.* **1**, 359–364 (2008).
12. Emanuel, K. A simple model of multiple climate regimes. *J. Geophys. Res.* **D 107**, 4077, doi:10.1029/2001JD001002 (2002).

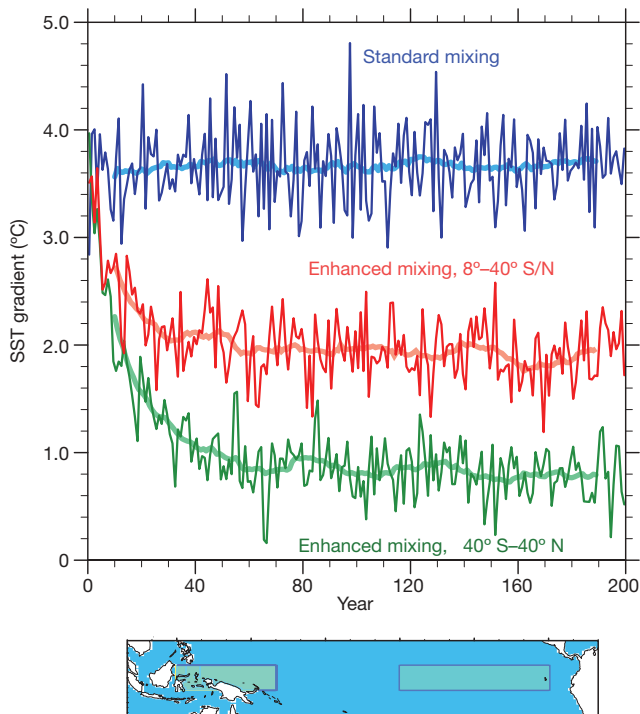


Figure 5 | Evolution of the equatorial SST gradient in three coupled experiments. The gradient is calculated as the difference in the annually averaged SSTs between the two regions in the western and eastern equatorial Pacific shown on the map at bottom. Thick lines correspond to 20-year running means. The increase in CO₂ alone from the preindustrial level to 355 p.p.m. does not change the equatorial gradient substantially (blue line). The increase in both CO₂ and ocean vertical mixing in the extra-tropical bands causes a 2 °C reduction in the equatorial gradient (red). Closing the equatorial gap reduces the SST gradient further to below 1 °C (green). The majority of these changes occur within the first 50 years of the simulations, and the adjustment of the upper ocean is almost completed by 100 years. The reduced variability in the two latter cases is indicative of a weaker El Niño/Southern Oscillation.

13. Korty, R. L., Emanuel, K. A. & Scott, J. R. Tropical cyclone-induced upper-ocean mixing and climate: application to equable climates. *J. Clim.* **21**, 638–654 (2008).
14. Robinson, M. M., Dowsett, H. J. & Chandler, M. A. Pliocene role in assessing future climate impacts. *Eos* **89**, 501–502 (2008).
15. Pagani, M., Lui, Z., LaRiviere, J. & Ravelo, A. C. High Earth-system climate sensitivity determined from Pliocene carbon dioxide concentrations. *Nature Geosci.* **3**, 27–30 (2010).
16. Thompson, R. S. & Fleming, R. F. Middle Pliocene vegetation: reconstructions, paleoclimatic inferences, and boundary conditions for climate modelling. *Mar. Micropaleontol.* **27**, 27–49 (1996).
17. Dowsett, H. J. *et al.* *Middle Pliocene Paleoenvironmental Reconstruction: PRISM2* 236 (Open File Rep. 99-535, USGS Geological Survey, 1999).
18. Haywood, A. & Valdes, P. Modelling Pliocene warmth: contribution of atmosphere, oceans and cryosphere. *Earth Planet. Sci. Lett.* **218**, 363–377 (2004).
19. Dowsett, H. J. & Robinson, M. M. Mid-Pliocene equatorial Pacific sea surface temperature reconstruction: a multi-proxy perspective. *Phil. Trans. R. Soc. A* **367**, 109–125 (2009).
20. Brierley, C. M. & Fedorov, A. V. The relative importance of meridional and zonal SST gradients for the onset of the Ice Ages and Pliocene-Pleistocene climate evolution. *Paleoceanography* doi:10.1029/2009PA001809 (in the press).
21. Brierley, C. M. *et al.* Greatly expanded tropical warm pool and weakened Hadley circulation in the early Pliocene. *Science* **323**, 1714–1718 (2009).
22. Dekens, P. S., Ravelo, A. C. & McCarthy, M. D. Warm upwelling regions in the Pliocene warm period. *Paleoceanography* **22**, doi:10.1029/2006PA001394 (2007).
23. Marlow, J., Lange, C., Wefer, G. & Rosell-Mele, A. Upwelling intensification as part of the Pliocene-Pleistocene climate transition. *Science* **290**, 2288–2291 (2000).
24. Haywood, A. M., Dekens, P., Ravelo, A. C. & Williams, M. Warmer tropics during the mid-Pliocene? Evidence from alkenone paleothermometry and a fully coupled ocean-atmosphere GCM. *Geochem. Geophys. Geosyst.* **6**, Q03010, doi:10.1029/2004GC000799 (2005).
25. D'Asaro, E. A. The ocean boundary layer below Hurricane Dennis. *J. Phys. Oceanogr.* **33**, 561–579 (2003).
26. Jacob, S., Shay, L., Mariano, A. & Black, P. The 3D oceanic mixed layer response to Hurricane Gilbert. *J. Phys. Oceanogr.* **30**, 1407–1429 (2000).
27. Woodruff, J. D., Donnelly, J. P., Emanuel, K. & Lane, P. Assessing sedimentary records of paleohurricane activity using modelled hurricane climatology. *Geochem. Geophys. Geosyst.* **9**, Q09V10, doi:10.1029/2008GC002043 (2008).
28. McCreary, J. & Lu, P. Interaction between the subtropical and equatorial ocean circulations — the subtropical cell. *J. Phys. Oceanogr.* **24**, 466–497 (1994).
29. Fedorov, A. & Philander, S. Is El Niño changing? *Science* **288**, 1997–2002 (2000).
30. Jansen, M. & Ferrari, R. Impact of the latitudinal distribution of tropical cyclones on ocean heat transport. *Geophys. Res. Lett.* **36**, L06604, doi:10.1029/2008GL036796 (2009).
31. Guilyardi, E. *et al.* Understanding El Niño in ocean-atmosphere general circulation models: progress and challenges. *Bull. Am. Meteorol. Soc.* **90**, 325–339 (2009).
32. Tziperman, E. & Farrell, B. Pliocene equatorial temperature: lessons from atmospheric superrotation. *Paleoceanography* **24**, PA1101, doi:10.1029/2008PA001652 (2009).

Supplementary Information is linked to the online version of the paper at www.nature.com/nature.

Acknowledgements We thank G. Philander, M. Barreiro, R. Pacanowski, C. Ravelo, P. deMenocal, T. Herbert, Y. Rosenthal, K. Lawrence, P. Dekens, A. Haywood, C. Wunsch and M. Huber for numerous discussions and encouragement. Financial support was provided by grants to A.V.F. from the NSF, the Department of Energy Office of Science, and the David and Lucile Packard Foundation. We thank B. Dobbins for help with computer simulations. This research used resources of the National Energy Research Scientific Computing Center.

Author Contributions A.V.F. and C.M.B. contributed equally to the writing and ideas in this paper. The original idea for this study belongs to A.V.F. C.M.B. conducted experiments with CAM3 and CCSM3. K.E. conducted calculations with the SDSM and provided expertise in the physics of tropical cyclones.

Author Information Reprints and permissions information is available at www.nature.com/reprints. The authors declare no competing financial interests. Correspondence and requests for materials should be addressed to A.V.F. (alexey.fedorov@yale.edu).

METHODS

The SST field used in GCM simulations for the Pliocene. The period of the SST distribution in Fig. 1b is around 4–4.2 million years ago, which coincides with the almost complete collapse of the east–west temperature gradient along the Equator in Fig. 1a. It is also after the closure of the Isthmus of Panama³³, and yet before climate cooled and large Northern Hemisphere ice sheets developed³⁴. The original temperature data are based on alkenone and Mg/Ca temperature proxies that have been adjusted to describe SSTs in the mid-Pacific approximately along the Date Line. For further details of the Pliocene SST distribution, see ref. 21. The modern SST profile shown in Fig. 1b is the average of 1961–90 from ref. 35.

The continuous SST profile used in boundary conditions for the atmospheric GCM takes the form:

$$T(\theta) = (T_{\max} - T_{\min}) \exp \left[-\frac{1}{a} \left(\frac{|\theta|}{45} \right)^N \right] + T_{\min} \quad (1)$$

where θ is the latitude in degrees, T_{\min} is the freezing temperature of sea water (set to 1.8 °C) and T_{\max} is the maximum temperature in the tropics (set to 28.5 °C). N is set to 4.5, while constant a is determined by a least-squares fit to the temperature estimates in Fig. 1b. The value of a differs in the Atlantic from the rest of globe to allow for warmer temperatures in the North Atlantic:

$$a = \begin{cases} 4.2 \Rightarrow 0 \leq \theta \leq 90, 270 \leq \phi \leq 360 \\ 2.6 \Rightarrow \text{otherwise} \end{cases} \quad (2)$$

where ϕ is the longitude in degrees east of Greenwich's prime meridian. To simulate the effect of the Peru Current along the coast of South America, which was warmer than at present but still colder than the surrounding waters²², we add a cold temperature anomaly, T_{Peru} , to our SST profile:

$$T_{\text{Peru}} = \begin{cases} -3 \cos^2 \left(\frac{\theta + 30}{30} \right) \cos^2 \left(\frac{\phi - 295}{30} \right) \Rightarrow -75 \leq \theta \leq 15, 250 \leq \phi \leq 295 \\ 0 \Rightarrow \text{otherwise} \end{cases} \quad (3)$$

Details of atmospheric GCM simulations. The atmosphere-only simulations were performed using the Community Atmosphere Model (CAM3³⁶) developed by the National Center for Atmospheric Research (NCAR). It is a three-dimensional spectral model of global extent, with 26 vertical levels and a horizontal truncation of T85. We also used CAM3 with the T42 resolution, which produced generally similar results (in particular, using data from the T42 model to drive the SDSM showed a similar shift in hurricane distribution but a smaller increase in the number of storms, ~20%).

The atmospheric model source code and the present day climatological boundary conditions are freely accessible on the Earth System Grid (<http://www.earthsystemgrid.org>). The modern simulation uses a similar set-up to that described in ref. 37. The model has been spun up for 15 months, after which it has reached dynamic equilibrium. The simulations are then integrated for another decade to create the input for the SDSM. Note that the resolution of the T42 model corresponds to ~2.8° transform grid; and the resolution of T85 to ~1.4° transform grid. The effective resolution of the downscaling model is <1 km, which is much smaller than that of the large-scale atmospheric GCMs.

For the early Pliocene run, we use the reconstructed SST profile as the surface boundary condition. The fractional sea ice cover was diagnosed from the SST. We have not included any other modifications to the boundary conditions, although changes did occur (such the extent of the Greenland ice sheet and a reduction in the height of the Rockies, Andes and Indonesia). Sensitivity studies have shown that the impact of the imposed SST profile on the Hadley circulation is an order of magnitude larger than the impact of other model modifications²¹.

Details of coupled GCM simulations. The coupled simulations are performed using the third version of NCAR's Community Climate System Model (CCSM3³⁸). This GCM incorporates the atmospheric component described above (CAM3) coupled to ocean and sea ice models (POP and CSIM, respectively). The model source code and the boundary conditions are freely accessible on the Earth System Grid (<http://www.earthsystemgrid.org>).

The two experiments discussed in this paper start from an equilibrated pre-industrial climate. The two runs are initialized with an instantaneous increase of atmospheric CO₂ concentrations to 355 p.p.m. (the level in 1990). For the first experiment (Fig. 4b), ocean background vertical diffusivity between 8° and 40° of latitude is increased by a factor of 10 in the top 200 m. This brings ocean diffusivity in the two bands on each side of the Equator to values ~1 cm² s⁻¹, which is consistent with the estimates of ref. 3.

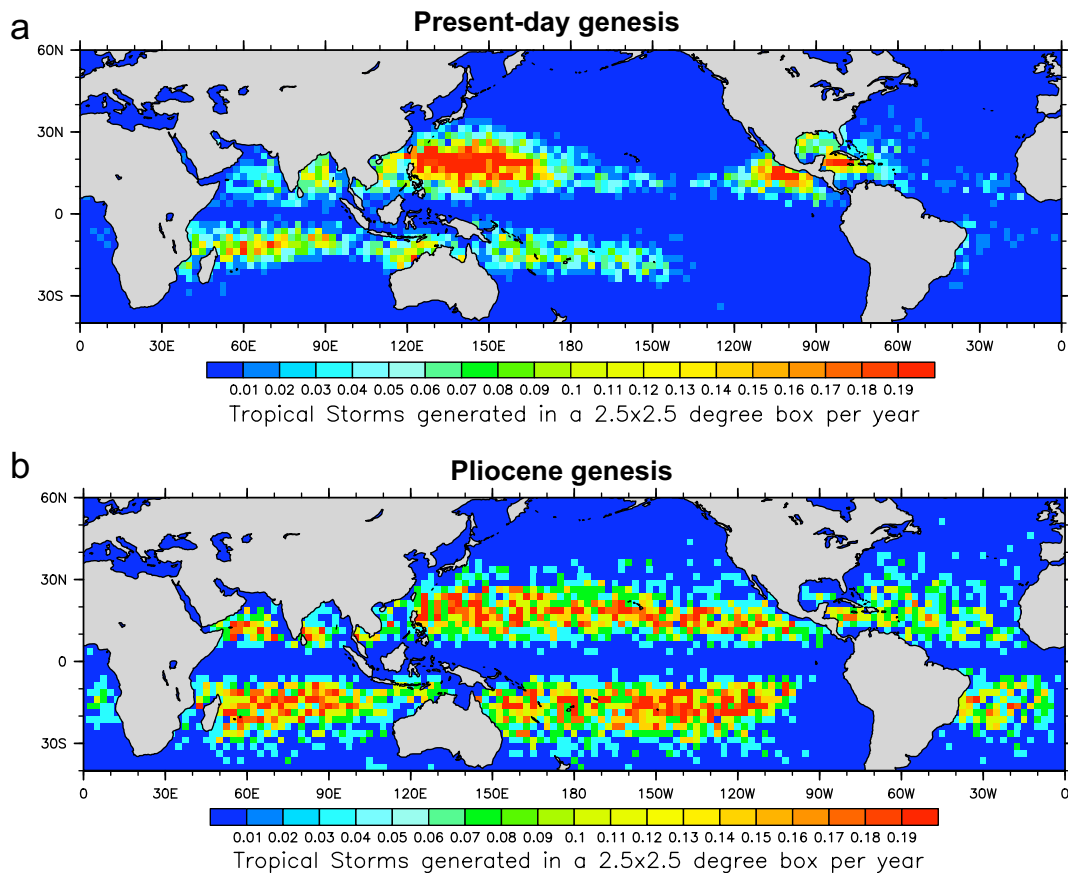
The methodology we use here is perhaps the simplest way to treat the impact of tropical cyclones. In reality, tropical cyclones are distributed very unevenly both in space and time. This makes deriving accurately the effective vertical diffusivity from a tropical cyclone distribution a non-trivial task with many uncertainties. A comprehensive study of these issues is now under way.

Our coupled experiments are similar to the recent work using an ocean-only simulation³⁰. Whereas those authors found a reduction in the ocean poleward heat transport in response to the subtropical mixing, we find an increase. This difference could arise from their use of restoring boundary conditions, which prevents significant SST and salinity variations and does not allow the atmosphere to respond to ocean circulation changes.

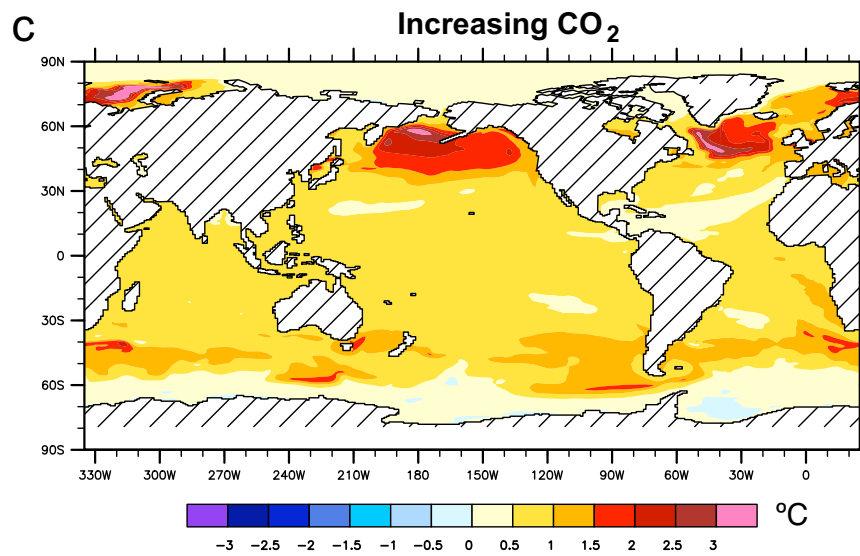
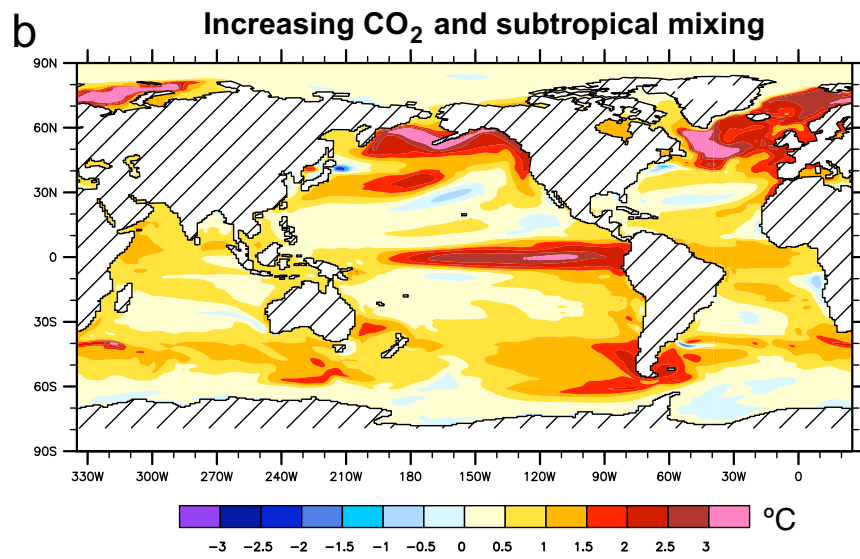
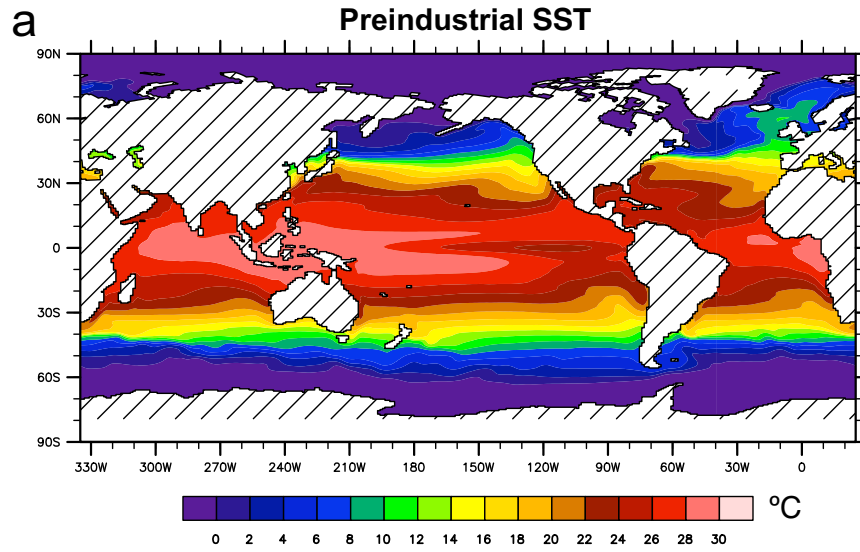
Our second experiment (Fig. 4c) utilizes the standard model set-up, used for instance in the IPCC Fourth Assessment Report³⁹. Both runs have been spun-up for 200 years, and an average of the last 20 years is chosen to make the comparison in Fig. 4.

33. Haug, G., Tiedemann, R., Zahn, R. & Ravelo, A. Role of Panama uplift on oceanic freshwater balance. *Geology* **29**, 207–210 (2001).
34. Zachos, J., Pagani, M., Sloan, L., Thomas, E. & Billups, K. Trends, rhythms, and aberrations in global climate 65 Ma to present. *Science* **292**, 686–693 (2001).
35. Rayner, N. A. *et al.* Global analyses of sea surface temperature, sea ice, and night marine air temperature since the late nineteenth century. *J. Geophys. Res.* **D 108**, 4407, doi:10.1029/2002JD002670 (2003).
36. Collins, W. D. *et al.* The formulation and atmospheric simulation of the Community Atmosphere Model: CAM3. *J. Clim.* **19**, 2144–2161 (2006).
37. Hack, J. J. *et al.* CCSM-CAM3 climate simulation sensitivity to changes in horizontal resolution. *J. Clim.* **19**, 2267–2289 (2006).
38. Collins, W. D. *et al.* The Community Climate System Model version 3 (CCSM3). *J. Clim.* **19**, 2122–2143 (2006).
39. Randall, D. A. *et al.* in *Climate Change 2007: The Physical Science Basis* (eds Susan, S. *et al.*) 589–662 (Cambridge Univ. Press, 2007).

MODELLED TROPICAL CYCLONE GENESIS

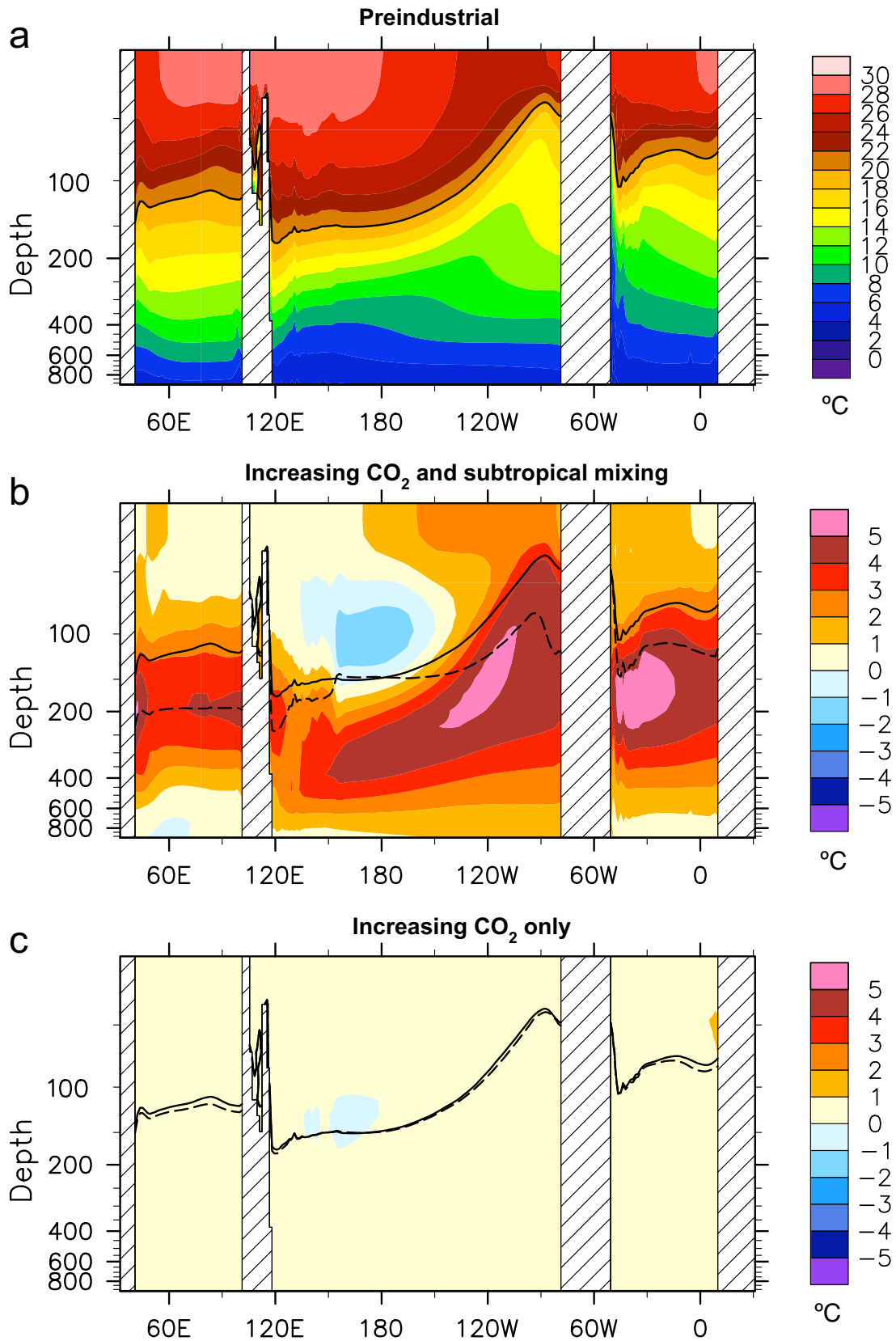


Supplementary Figure 1 | Modelled genesis of tropical cyclones: (a) The present-day climate. (b) The early Pliocene. The panels show the average number of tropical cyclones originating annually in each $2.5^\circ \times 2.5^\circ$ box in the Statistical DownScaling Model. The average number of tropical cyclones passing through each box is at least an order of magnitude larger. Note the expansion of the tropical cyclone activity and the overall increase in the number of cyclones during the Pliocene.



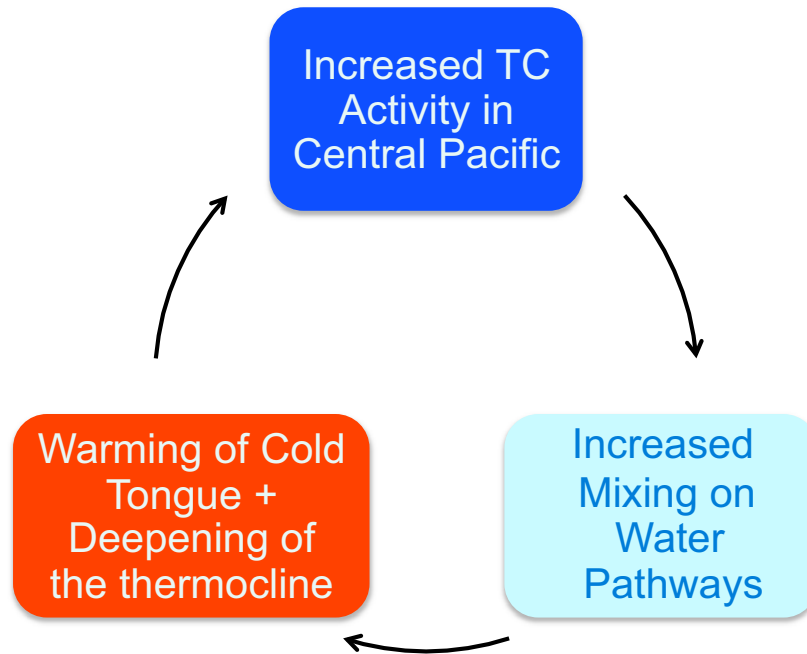
Supplementary Figure 2 | Global SST changes simulated in the coupled experiments. (a) Preindustrial climate conditions. (b) SST change in response to increasing atmospheric CO₂ concentration from 285ppm (preindustrial) to 355ppm (the level of 1990) and enhancing vertical diffusivity in the upper ocean in the extra-tropical bands after 200 years of calculations for the Pliocene scenario. The SST increase has a signature of permanent El Niño-like conditions with the maximum warming reaching 3.5°C in the eastern equatorial Pacific. (c) SST changes in response to increasing CO₂ concentration alone. Note the warming of the Northern Pacific and Atlantic. This warming is stronger in the experiment with enhanced ocean mixing when it can reach ~5°C. A moderate cooling off South-West Africa in (b) is caused by prescribing too strong diffusivity near the coast, which is not supported by the PDI distribution in Fig. 3.

TEMPERATURE ALONG THE EQUATOR



Supplementary Figure 3 | Ocean thermal structure along the equator in the coupled simulations (averaged between 5°S-5°N). (a) Ocean temperature for preindustrial climate conditions. (b) Temperature changes in response to increasing atmospheric CO₂ concentration from 285ppm (preindustrial) to 355ppm (the level of 1990) and enhancing vertical diffusivity in the upper ocean in the extra-tropical bands after 200 years of calculations for the Pliocene scenario. (c) Temperature changes in response to increasing CO₂ concentration alone. The solid black lines in all panels show the depth of the 20°C isotherm, a proxy for the thermocline depth, in the preindustrial simulation. The dashed lines show the 20°C isotherm in the perturbed experiments. Note the deepening of the thermocline in all three oceans caused by the enhanced extra-tropical mixing, as well as the reduction of the thermocline slope in the Pacific related to the Bjerknes feedback. Also note the strong warming (up to 6°C) below the thermocline, especially in the Pacific and Atlantic oceans, and a moderate subsurface cooling (1-2°C) in the western Pacific.

Ocean Circulation - Tropical Cyclone Feedback



Supplementary Figure 4 | Schematic of the positive climate feedback based on interaction between ocean circulation and tropical cyclones.